Desalination and Water Treatment
www.deswater.com
doi: 10.5004/dwt.2022.28340

255 (2022) 185–191
April

Elaboration and characterization of new polymeric membrane based on cellulose triacetate, polyelectrolytes and dioctylephthalate as plasticizer

Nesrine Drai[a], Naima Abdellaoui[b], Faouzi Saib[c,d], Omar Arous[a,*], Mohamed Trari[c]

[a]*Laboratory of Hydrometallurgy and Inorganic Molecular Chemistry, Faculty of Chemistry, USTHB, P.O. Box: 32 ELAlia Babezzouar, 16111 Algeria, emails: omararous@yahoo.fr (O. Arous), drainesrine@gmail.com (N. Drai)*
[b]*Laboratory of Polymer Materials, Faculty of Chemistry, USTHB, P.O. Box: 32 ELAlia Babezzouar, 16111 Algeria, email: naima.abdellaoui1973@gmail.com*
[c]*Laboratory of Storage and Valorization of Renewable Energies, Faculty of Chemistry, USTHB, P.O. Box: 32 ELAlia Babezzouar, 16111 Algeria, email: solarchemistry@gmail.com*
[d]*Center of Research in Physical and Chemical Analysis, CRAPC, Bousmail Tipaza, Algeria, email: saib.dz@gmail.com*

Received 13 August 2021; Accepted 27 December 2021

ABSTRACT

In this paper work, polymer solutions of cellulose triacetate and dioctylephthalate mixed with polyelectrolytes: polyacrylic acid, polyvinylpyrrolidone and polyvinyl alcohol were used to make selective polymeric membranes by the phase inversion technique via immersion precipitation. The impact of a polyelectrolytes additive on the structure and performances of the membranes was studied. The achieved membranes were characterized by thermogravimetric analysis, Fourier-transform infrared spectroscopy–attenuated total reflection, scanning electron microscopy and contact angle measurements. As the plasticizer molecules were hydrophobic, their location at the surface of the improved polymeric membranes is expected to adapt the contact angle. Overall, our results show that the addition of plasticizer to the new material results in homogeneous and hydrophobic membranes of which the physical properties were enhanced compared to the commercial membranes. In a second part, we have successfully synthesized new photo-electrodes: *n*-$Sr_2Fe_2O_5$ and *p*-$CuFeO_2$ and their photo-electrochemical characterizations are recognized. The transport of cadmium ions (Cd^{2+}) using combined membranes with semiconductors is studied as application.

Keywords: Polymers; Organic membranes; Heavy metals; Water purification; Semiconductors

1. Introduction

Heavy metals (specifically cadmium) have accruing characteristics in nature as they cannot be biodegraded [1]. In spite of its harmfulness, cadmium is used in different industries such as tinctures, electroplating, metallurgical products, etc. Most regularly, cadmium could attain the water system through industrial release. Consequently, its elimination from several effluents had attracted considerable attention from the scientific and technological points of view.

Cadmium can be eliminated from wastewater by using numerous physical and chemical techniques like adsorption, chemical settling, reverse osmosis and solvent extraction which are the most commonly used methods. Conventional methods for heavy metal removal also include chemical precipitation, electrolytic recovery, electrodialysis, ion-exchange

* Corresponding author.

Presented at the International Virtual Conference on Water and Energy (ICWE 21), Hassiba Benbouali University of Chlef, Algeria, 25–27 May 2021

resin, liquid-liquid extraction and liquid membrane (LM) separation [2].

During the previous years, solvent extraction of cadmium from various aqueous media has involved specific interest and diverse components have been considered, including acidic, basic and neutral complexants and some of their mixtures [3–10]. Among these, LM has received considerable attention in the past three decades due to its characteristics such as simplicity of operation, energy and selectivity advantages as well as low cost operation factors [11,12]. However, the principal handicaps with using liquid membranes are the low fluxes, the discharge of the carrier and insufficient physical stability. These problems as well as others have prohibited wide-scale application of liquid membranes in industrial separations [13,14].

Later, new generation of ion exchange membranes has been elaborated when the hydrophilic and hydrophobic equilibrium is changed. Polymer inclusion membranes (PIMs) have been efficaciously used in some areas such as biochemistry, agronomy, chemistry, medicine, pharmaceuticals, water treatment and fine chemical separations principally in nuclear industry [15–18]. The selective separation of this kind of polymeric membranes is accomplished frequently by the presence of selective compounds, called carriers, in the membrane phase. The carriers are responsible to facilitate the transport of the target component across the selective membrane. This phenomenon is termed facilitated transport and has been the subject of numerous articles [19–27].

On the other hand, numerous semiconductors have been magnificently used for solar energy conversion [28–30]. The electron-transfer reactions are essentially governed by local electrostatic potential gradients through the interfaces [31]. In the liquid junctions, the electric field developed in the space charge region hinders the recombination of charge carriers formed by light excitation [32]. The kinetic in such system is difficult to monitor and no detailed study has been reported before now [33].

In this paper, we have synthesized new polymer inclusion membranes (PIMs) using cellulose triacetate (CTA) and three polyelectrolytes: polyacrylic acid noted (PAA), polyvinylpyrrolidone noted (PVP) or polyvinyl alcohol noted (PVA). All synthesized membranes are plasticized by dioctylephthalate (DOP). The synthesized membranes were characterized by Fourier-transform infrared spectroscopy (FTIR), thermogravimetric analysis (TGA), scanning electron microscopy and contact angle. In a second part, we have elaborated two new semiconductors: *n*-$Sr_2Fe_2O_5$ and *p*-$CuFeO_2$ and their photo-electrochemical characterizations are undertaken. As application, the transport of Cd^{2+} using synthesized membranes coupled with the photo-electrodes is studied.

2. Materials and methods

2.1. Chemicals

All chemicals were of analytical reagent grade. $CdCl_2$ (99.99%), chloroform ($CHCl_3$) (pure), cellulose triacetate (CTA) (pure), polyacrylic acid (PAA), polyvinylpyrrolidone (PVP) and polyvinyl alcohol (PVA) are analytical grade reagents acquired from Fluka. Dioctyl phthalate (RPE ≥ 99, 5%) was product of CARLO ERBA. All reagents were used as received without any further purification. To prepare the aqueous solutions the different reagents were dissolved in deionized water.

2.2. Preparation of polymeric membranes

Polymer inclusion membranes were prepared using a new method and according to the previous study [34,35]. 0.4 g of cellulose triacetate (CTA) and 0.2 g of polyelectrolyte were dissolved in 40 mL of chloroform and stirred for 4 h. Then, 0.2 mL of DOP was added under vigorous stirring during 2 h. After a homogenous mixture was obtained, the miscible solution was transferred to circular glass containers and the solvent was slowly and completely evaporated in an oven at 60°C. The formed membrane was detached from the Petri glass by immersion in cold water.

2.3. Synthesis of $Sr_2Fe_2O_5$ and $CuFeO_2$ semi-conductors

The brownmillerite $Sr_2Fe_2O_5$ was prepared by nitrate route from $Fe(NO_3)_3$ $9H_2O$ (Merck, 99.5%) and $Sr(NO_3)_2$ (Merck, >99.5%). The stoichiometric mixture was dissolved in water and the solution is slowly evaporated on a sand bath. The powder was ground, pressed into pellets and heated at 750°C for 10 h, the compactness averages 75%. The delafossite $CuFeO_2$ is synthesized by nitrate decomposition; the detailed preparation procedure is given elsewhere [33]. The powder is ground, pressed into pellets and fired at 950°C for 8 h (120°C/h) to have good mechanical properties. The end product exhibits a blue color and the compactness approximates 80%.

2.4. Analysis

FTIR spectra are recorded using a Perkin-Elmer spectrometer (Spectrum One). The apparatus was standardized before analysis with 60 scans at a resolution fixed to 2 cm^{-1} in the wavenumber range of 4,000–400 cm^{-1}. TGA analyses were realized using a TGA Q500, TA Instrument, programmed from 50°C to 600°C at a rate of 10°C/min. All samples were purged with N_2 gas at a flow rate of 60 mL min^{-1}. The cadmium(II) concentrations in all compartments (alimentation and reception solutions) were determined at different time intervals (1 h) using the atomic absorption spectroscopy method (AAS) with a Perkin-Elmer spectrometer Analyst AA-700 model.

2.5. Membrane transport experiments

Ions transfer experimentations were carried out in a permeation cell consisting of three identical cylindrical compartments (100 cm^3 capacity). The synthesized membranes with an active area of 9.61 cm^2 was inserted between three compartments, sealed with silicon, and tightly clamped. The same volume of aqueous solutions were injected into the three compartments as feed phase (A) and strip phases (B and C) respectively. The same volume of aqueous solutions were injected into the feed and strip phases respectively. All experiments were performed at the setting temperature. In order to study the transport

dynamics, 0.5 mL samples were collected from the two phases at pre-selected time (1 h) and analyzed by AAS.

3. Results and discussion

3.1. Characterization of the elaborated polymeric membranes by FTIR

The membranes CTA + polyelectrolyte + plasticizer were characterized by FTIR technique. Fig. 1 shows the FTIR spectra of PVPM (CTA + PVP + DOP), PVAM (CTA + PVA + DOP) and PAAM (CTA + PAA + DOP) membranes.

The FTIR spectra of all synthesized membranes show several bands in (2,960–2,850 cm^{-1}) region attributed to elongation vibrations of the asymmetric and symmetric C–H bonds respectively. The main features of these spectra are the absorption band located around 1,752 cm^{-1}, attributed to stretching vibrations of the carbonyl group (C=O) of CTA, DOP and PAA components. The PVPM membrane spectrum also revealed another band localized at around 1,663 cm^{-1}, characteristic of the carbonyl group of PVP polymer. This peak initially present at 1,654 cm^{-1} in the pure component shifted to higher wavenumbers in this membrane.

The presence of hydroxyl groups (O–H) of CTA, PVA and PAA polymers was confirmed by the wide band at 3,476 cm^{-1}. Bands detected at 1,225 and 1,041 cm^{-1} correspond respectively to the asymmetric and symmetric stretching modes of C–O–C single bonds of CTA and DOP.

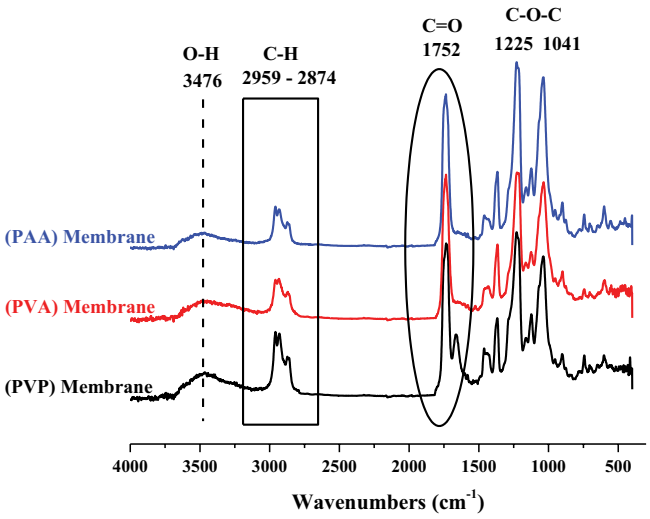

Fig. 1. FTIR spectra of different synthesized membranes.

3.2. Characterization of the elaborated polymeric membranes by TGA

Fig. 2 shows the weight loss thermograms TGA, and the corresponding first derivatives d(TGA) curves of pure polymers CTA, PVP, PVA and PAA, obtained by conventional TGA.

As it can be seen from this figure, after a slight loss of weight at a range of temperature of 25°C–250°C, due to the elimination of water molecules absorbed by the hydrophilic groups of the used polymers, the degradation process of CTA, PVP and PAA contains a single step of degradation while the PVA degrades in two main stages.

The dTG thermogram of PAA exhibits also an additional peak at about 243°C attributed to the formation of anhydrides after elimination of water molecules from PAA polymeric chains. This phenomenon was confirmed in the literature [36–38]. The main stage of degradation of PAA occurs at a temperature range of [301°C–465°C], where this polymer loses 89% of its initial mass giving a small residue of 1%. The T_{max}, determined from the maximum of the peak of the first derivative curve as a function of the temperature d(TGA), is noted at about 399°C. This step of degradation is attributed to the decomposition of the previously formed polyanhydride.

A significant weight loss of about 85 wt.% was observed for CTA from 300°C to 433°C. This step of degradation with a residue of 12 wt.%, is attributed to the elimination of all

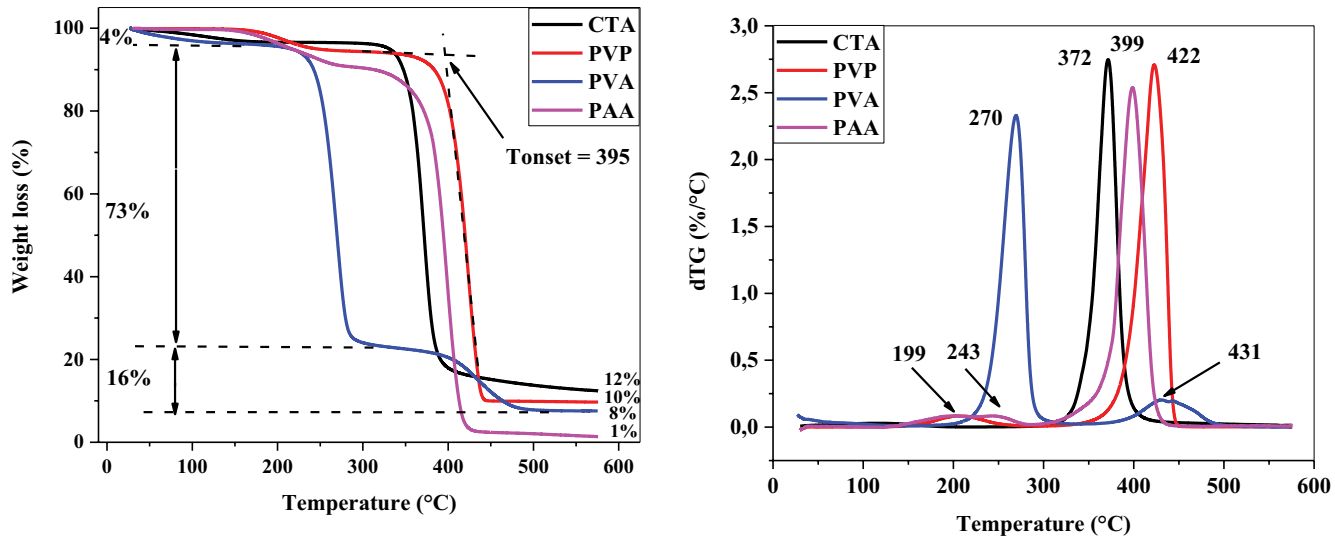

Fig. 2. Thermogravimetric analysis (TGA) and d(TGA) curves of CTA, PVP, PVA and PAA polymers.

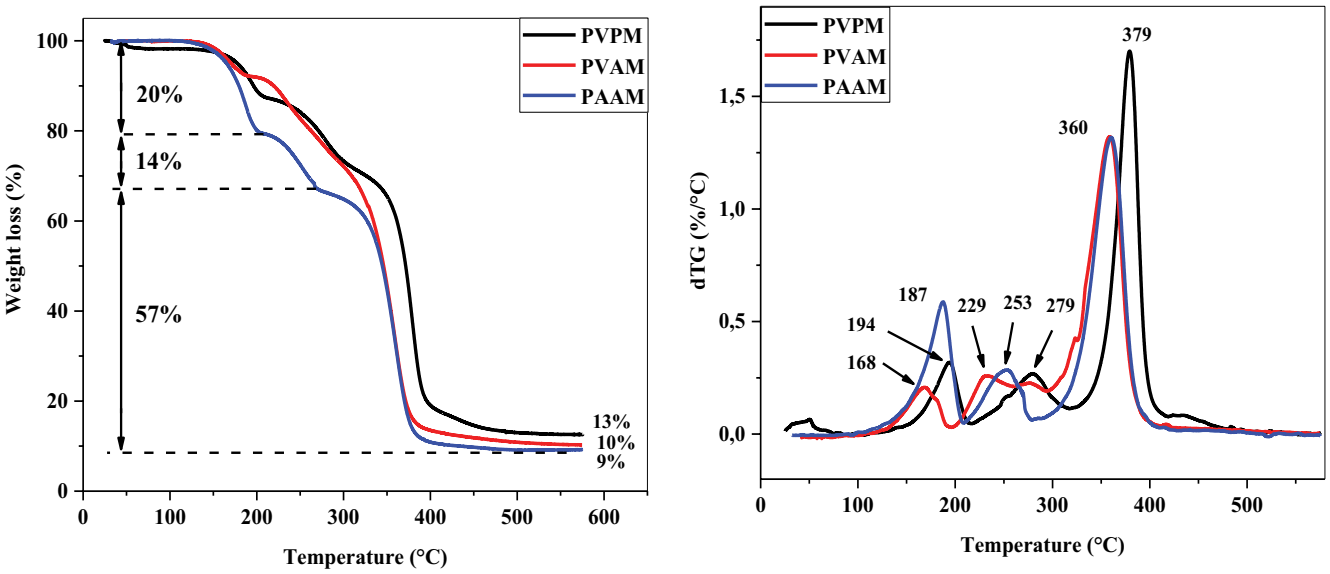

Fig. 3. Thermogravimetric analysis (TGA) and d(TGA) curves of synthesized membranes.

the acetate groups and the formation of pyranose ring in the CTA polymer. The onset temperature of degradation (T_{onset}), determined by drawing tangents, is about 355°C while the degradation temperature at maximum rate T_{max} is observed at 372°C for this polymer.

The single stage of degradation of PVP occurs at a temperature range of [312°C–465°C] with a weight loss of 84% and a residue of 10 wt.%. The T_{onset} and the T_{max} were about 395°C and 421°C, respectively.

The thermal degradation behaviour of PVA shows an important weight loss of about 73% at a temperature range of [190°C–330°C]. This stage with T_{onset} of 251°C and T_{max} of 270°C, is due to partial dehydration of PVA chains leading to polyene formation followed by polyene decomposition. In the last stage between 359°C and 501°C, the mass loss was about 15% and the residual percentage of the weight was equal to 8%. This step of degradation is attributed to the carbonization process.

Fig. 3 exhibits the weight loss thermograms TGA and the corresponding derivatives d(TGA) curves of synthesized membranes PVPM (CTA + PVP + DOP), PVAM (CTA + PVA + DOP) and PAAM (CTA + PAA + DOP).

From these thermograms we can note that, PVPM and PAAM membranes degrade in three main stages while the PVAM one exhibits four main steps of degradation.

During the first one that occurred over a temperature range of 112°C–215°C, the PVPM membrane lost about 11 wt.% of its initial mass with a T_{max} at 194°C and a T_{onset} at 173°C. This stage of degradation is probably due to the evaporation of the plasticizer DOP which is characterised by an ebullition temperature of 220°C. After that, this membrane displayed another weight loss of 16% in a temperature domain of [219°C–318°C] with T_{max} at 279°C. This step of degradation is probably attributed to the evaporation of the remaining plasticizer (DOP) hydrogen bonded with a small amount of CTA polymer. Finally, PVPM membrane thermogram exhibits the most important weight loss of about 58% with T_{max} at 379°C. This step is characteristic of the degradation of the two inter-associated polymers (CTA and PVP).

The degradation process of the membrane PVAM (CTA + PVA + DOP) follows four main stages. This membrane exhibits a thermal stability up to 105°C. A mass loss of about 8 wt.% was recorded during the first step of degradation which extends over a temperature range of 103°C–194°C with a T_{max} of around 168°C and T_{onset} of 144°C. This stage is attributed to the evaporation of a part of the plasticizer DOP. During the second stage of degradation, ranging from 198°C to 256°C, the membrane PVAM lost 11% of its mass with a T_{max} at 230°C. This weight loss is characteristic of the degradation of the remaining DOP hydrogen bonded with the CTA and the PVA polymers. The third degradation stage of this membrane with a T_{max} of 277°C is attributed to the degradation of PVA polymer. This step is easily detectable in the thermogram of pure PVA. Finally the most important weight loss of this membrane of about 62%, recorded at T_{max} of 359°C is due to the degradation of the two inter-associated polymers (CTA and PVA).

The degradation process of the last membrane PAAM (CTA + PAA + DOP) occurs in three main steps. The first one, attributed to the evaporation of a part of the plasticizer DOP and to the elimination of water molecules from PAA chains, extends over a temperature range from 110°C–203°C. During this stage of degradation, the membrane lost 20 wt.% of its initial mass with T_{max} at around 187°C and T_{onset} at 166°C.

The second and the third steps of degradation with weight loss of 13% and 57% respectively and T_{max} of 253°C and 360°C respectively are attributed to the evaporation of DOP and the degradation of the two inter-associated polymers.

Based on the values of T_{onset} of elaborated membranes, all the membranes exhibited a thermal stability until 144°C (T_{onset} of PVPM = 173°C, T_{onset} of PVPA = 144°C and T_{onset} of PAAM = 166°C). This temperature is much higher than that required in the membrane processes. It is also clear that the

PVPM membrane is the most thermally stable one with T_{onset} of 173°C.

3.3. Transport of cadmium ions using a synthetic membranes

The nature of the illumination source is studied using $Sr_2Fe_2O_5$ and $CuFeO_2$ as polarized electrodes in the extremities of each membrane. The dependence of the ionic membrane nature has been studied using two supports of different chemical and physical characteristics; (CTA + PVP + DOP) as cationic membrane and (CTA + PVA + DOP) as anionic membrane. We used also *n*-$Sr_2Fe_2O_5$ and *p*-$CuFeO_2$ in short circuited configuration to ensure creation of electrical field as transference gradient forces. The photo-electrodeposition catalyzes the diffusion process as evidenced from the Cd^{2+} concentrations. Consequently, the equilibrium strongly lies to the right hand, that is, the Cd deposition according to the Le Chatelier principle. This system is applied after the separation and transport across a polymer inclusion membrane (PIM) modified by the semiconductors (Fig. 4).

Figs. 5 and 6 give the variation of Cd^{2+} concentration in feed and strip compartments vs. the nature of the illumination source.

Figs. 5 and 6 show that the quantities of Cd^{2+} ions decrease strongly in the feed compartment by passing from the cationic membrane thus confirming that the transport of metallic ions is an active transport, where charges number of the polyelectrolyte plays an important role in the process. We note also a plateau region is reached after 5 h with a percentage of 31% using a solar illumination source. Such result shows that among 69% of Cd^{2+} transferred to the cathodic compartment, with 48% free and 21% have undergone a reduction to metallic state.

In the case of LED lamp source, nearly the same percentage (40%) of no transferred cadmium is obtained after 6 h of illumination. This indicates that 60% of cadmium ions

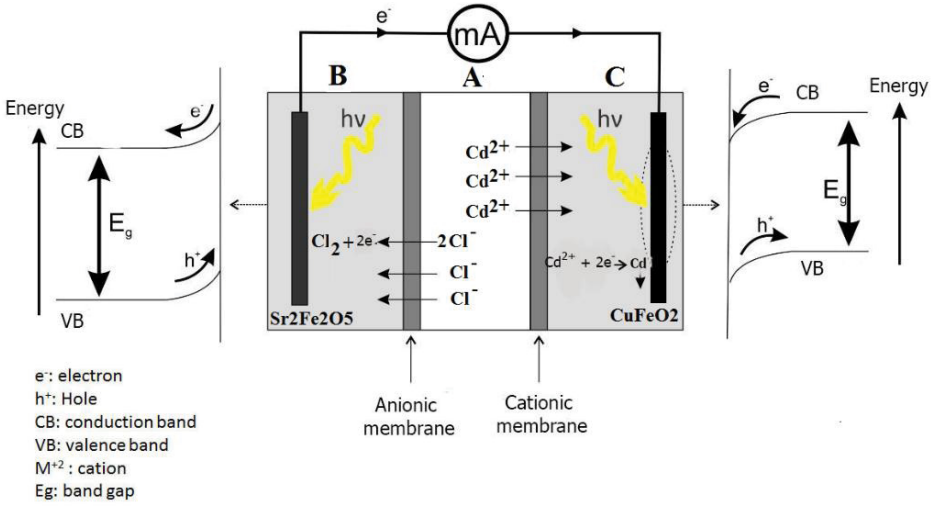

Fig. 4. Photo-electrodialysis cell: (anode) $Sr_2Fe_2O_5$; (cathode) $CuFeO_2$.

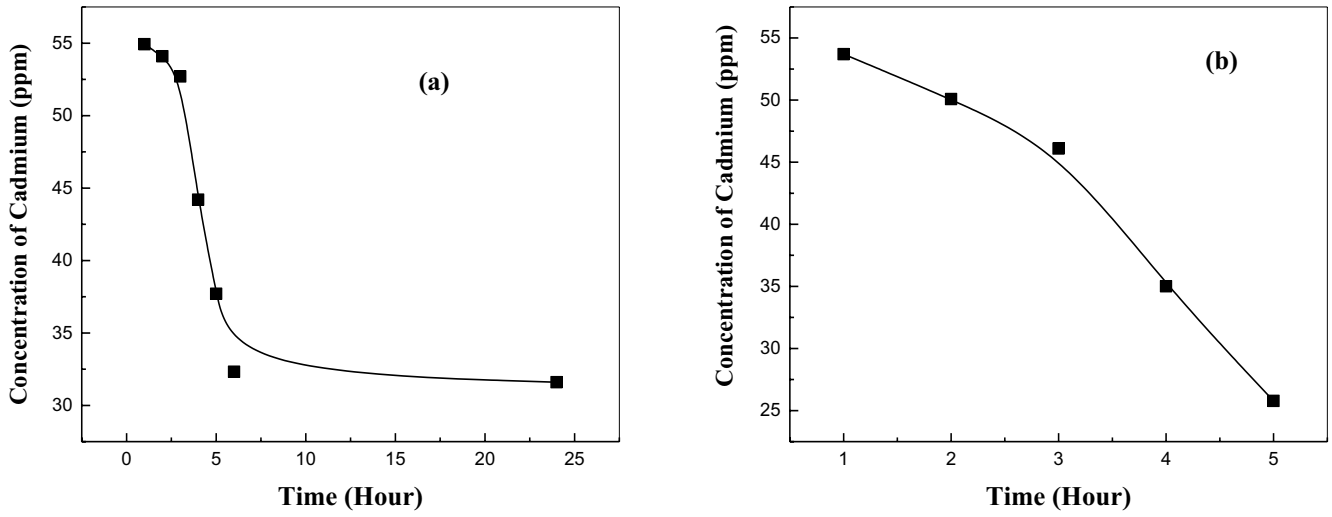

Fig. 5. Evolution of the concentration of cadmium in the feed phase vs. time using (a) LED lamp illumination and (b) solar illumination, $[Cd^{2+}]_0$ = 80 ppm.

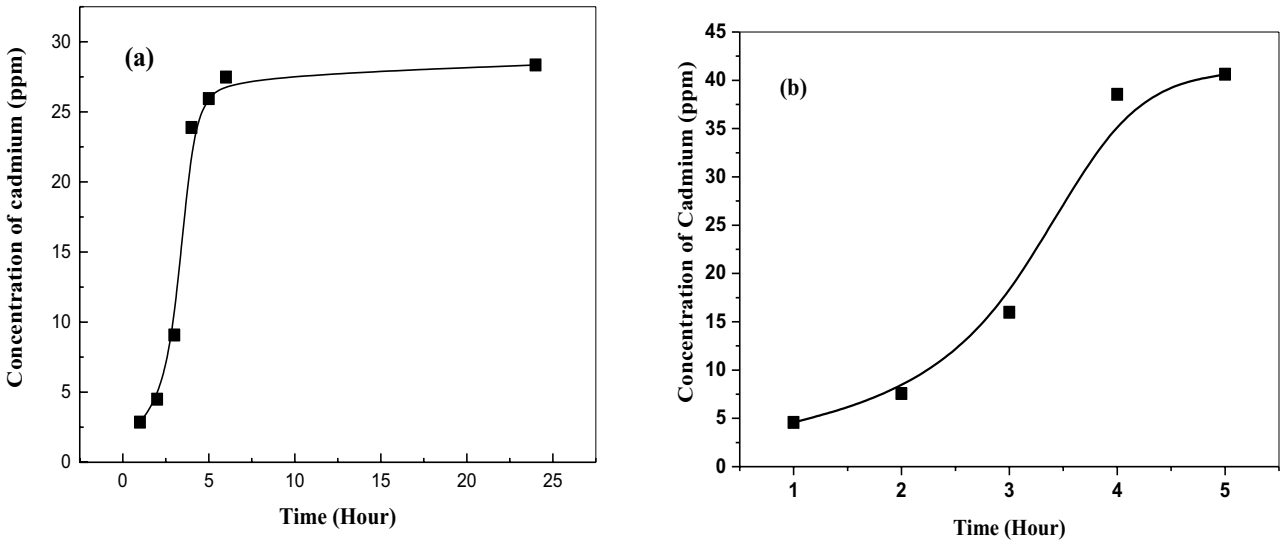

Fig. 6. Evolution of the concentration of cadmium in the strip phase vs. time using (a) LED lamp illumination and (b) solar illumination, $[Cd^{2+}]_0$ = 80 ppm.

were transferred toward the feed compartment (35% free and 25% reduced into Cd^0).

4. Conclusion

The present paper combined the electrochemical reactions caused by solar energy with polymeric membranes process for metallic ions elimination. Cellulose triacetate membranes modified by poly-electrolytes and containing dioctylephthalate (DOP) as plasticizer have been successfully elaborated. These polymers + plasticizer + polyelectrolyte membranes were characterized using FTIR, TGA and XRD analysis. Our approach was to use n/p semiconductors in a short circuited configuration to generate an electrical field as transference gradient force. This system was applied to the light-driven reduction of cadmium, after the separation and transport across a polymer inclusion membrane (PIM) in combination with semiconductors (*n*-$Sr_2Fe_2O_5$ and *p*-$CuFeO_2$). The results showed that the Cd^{2+} photo-electrodeposition was significantly increased when using modified PIMs by photo-electrode. It has also been shown an increase of the diffusion flux when the electrode was activated by solar illumination.

References

[1] S. Veli, B. Alyüz, Adsorption of copper and zinc from aqueous solutions by using natural clay, J. Hazard. Mater., 149 (2007) 226–233.
[2] G L. Rorrer, Heavy Metal Ions, Removal From Wastewater, R.A. Meyers, Eds., Encyclopedia of Environmental Analysis and Remediation, Wiley, New York, 1998, pp. 2102–2125.
[3] L.-C. Li, R.-S. Juang, Ion-exchange equilibria of Cu(II) and Zn(II) from aqueous solutions with Chelex 100 and Amberlite IRC 748 resins, Chem. Eng. J., 112 (2005) 211–218.
[4] C.A. Nogueira, F. Delmas, New flowsheet for the recovery of cadmium, cobalt and nickel from spent Ni–Cd batteries by solvent extraction, Hydrometallurgy, 52 (1999) 267–287.
[5] B. Wassink, D. Dreisinger, J. Howard, Solvent extraction separation of zinc and cadmium from nickel and cobalt using Aliquat 336, a strong base anion exchanger, in the chloride and thiocyanate forms, Hydrometallurgy, 57 (2000) 235–252.
[6] S. Memon, M. Yilmaz, Biscalixarenes: synthesis and investigation of the extraction behaviour of biscalix[4]arene derivatives in a two-phase extraction system, Sep. Sci. Technol., 36 (2001) 473–486.
[7] B. Gupta, A. Deep, P. Malik, Extraction and recovery of cadmium using Cyanex 923, Hydrometallurgy, 61 (2001) 65–71.
[8] K. Takeshita, K. Watanabe, Y. Nakano, M. Watanabe, Solvent extraction separation of Cd(II) and Zn(II) with the organophosphorus extractant D2EHPA and the aqueous nitrogen-donor ligand TPEN, Hydrometallurgy, 70 (2003) 63–71.
[9] K. Takeshita, K. Watanabe, Y. Nakano, M. Watanabe, Extraction separation of Cd(II) and Zn(II) with Cyanex 301 and aqueous nitrogen-donor ligand TPEN, Solvent Extr. Ion Exch., 22 (2004) 203–218.
[10] Q. Jia, CH. Zhan, DQ. Li, CJ. Niu, Extraction of zinc(II) and cadmium(II) by using mixtures of primary amine N1293 and organophosphorus acids, Sep. Sci. Technol., 39 (2004) 1111–1123.
[11] F.J. Alguacil, Mechanistic study of active transport of copper(II) from ammoniacal/ammonium carbonate medium using LIX 973N as a carrier across a liquid membrane, Hydrometallurgy, 61 (2001) 177–183.
[12] P. Venkateswaran, K. Palanivelu, Recovery of phenol from aqueous solution by supported liquid membrane using vegetable oils as liquid membrane, J. Hazard. Mater., 131 (2006) 146–152.
[13] A. Gherrou, H. Kerdjoudj, R. Molinari, E. Drioli, Facilitated transport of Ag(I), Cu(II) and Zn(II) ions by using DB18C6 and DA18C6 as carriers: interface behaviour on the ion transport, Sep. Sci. Technol., 36 (2001) 2289.
[14] C. Hill, J.-F. Dozol, H. Rouquette, S. Eymard, B. Tournois, Study of stability of some supported liquid membranes, J. Membr. Sci., 114 (1996) 73–80.
[15] A.K. Pabby, S.S.H. Rizvi, A.M. Sastre, Handbook of Membrane Separations Chemical, Pharmaceutical, Food and Biotechnological Applications, CRC Press, Taylor & Francis Group, 6000 Broken Sound Parkway NW, 2009.
[16] H. Inoue, M. Kagoshima, M. Yamasaki, Y. Honda, Radioactive iodine waste treatment using electrodialysis with an anion exchange paper membrane, Recent Adv. Multidisciplinary Appl. Phys., 61 (2005) 795–803.
[17] K. Maiphetlho, L. Chimuka, H. Tutu, H. Richards, Technical design and optimisation of polymer inclusion membranes

(PIMs) for sample pre-treatment and passive sampling – a review, Sci. Total Environ., 799 (2021) 149483, doi: 10.1016/j.scitotenv.2021.149483.
[18] D. Bożejewicz, K. Witt, M.A. Kaczorowska, The comparison of the removal of copper(II) and zinc(II) ions from aqueous solution using 2,6-diaminopyridine in a polymer inclusion membrane and in a classic solvent extraction, Desal. Water Treat., 214 (2021) 194–202.
[19] M. Akhond, M. Shamsipur, Specific uphill transport of Cd2C ion by a cooperative carrier composed of containing aza-18-crown-6 and palmitic acid, J. Membr. Sci., 117 (1996) 221–226.
[20] A.J. Schow, R.T. Peterson, J.D. Lamb, Polymer inclusion membranes containing macrocyclic carriers for use in cation separations, J. Membr. Sci., 111 (1996) 291–295.
[21] T. Fyles, Polymer Membrane for Proton Driven Ion Transport, 1990 U.S. Patent 4,906,376.
[22] E.L. Cussler, R. Aris, A. Brown, On the limits of facilitated diffusion, J. Membr. Sci., 43 (1989) 149–164.
[23] R.D. Noble, Generalized microscopic mechanism of facilitated transport in fixed site carrier membranes, J. Membr. Sci., 75 (1992) 121–129.
[24] P. Lacan, C. Guizard, P.L. Gall, D. Wettling, L. Cot, Facilitated transport of ions through fixed-site carrier membranes derived from hybrid organic–inorganic materials, J. Membr. Sci., 100 (1995) 99–109.
[25] Y.S. Kang, J.-M. Hong, J. Jang, U.Y. Kim, Analysis of facilitated transport in solid membranes with fixed site carriers. 1. Single RC circuit model, J. Membr. Sci., 109 (1996) 149–157.
[26] J.M. Hong, Y.S. Kang, J. Jang, U.Y. Kim, Analysis of facilitated transport in polymeric membrane with fixed site carrier. 2. Series RC circuit model, J. Membr. Sci., 109 (1996) 159–163.
[27] J.D.W. McBride, R.M. Izatt, J.D. Lamb, J.J. Christensen, Inclusion Compounds III, Academic Press, London, 1984, pp. 571–628.
[28] C. Belabed, N. Haine, Z. Benabdelghani, B. Bellal, M. Trari, Photocatalytic hydrogen evolution on the hetero-system polypyrrol/TiO_2 under visible light, Int. J. Hydrogen Energy, 39 (2014) 17533–17539.
[29] D. Meziani, K. Abdelmeziem, S. Bouacida, M. Trari, Photo-electrochemical and physical characterizations of a new single crystal POM-based material. Application in photocatalysis, J. Mol. Struct., 1125 (2016) 540–545.
[30] D. Meziani, K. Abdelmeziem, S. Bouacida, M. Trari, H. Merazig, Photo-electrochemical and physical characterizations of a new single crystal POM-used material. Application to Rhodamine B photodegradation, Sol. Energy Mater. Sol. Cells, 147 (2016) 46–52.
[31] G. Rekhila, Y. Bessekhouad, M. Trari, Hydrogen evolution under visible light over the solid solution $NiFe_{2-x}Mn_xO_4$ prepared by sol–gel, Int. J. Hydrogen Energy, 40 (2015) 12611–12618.
[32] B. An, T.R. Steinwinder, D. Zhao, Selective removal of arsenate from drinking water using a polymeric ligand exchanger, Water Res., 39 (2005) 4993–5004.
[33] S. Omeiri, Y. Gabes, A. Bouguelia, M. Trari, Photo-electrochemical characterization of the delafossite $CuFeO_2$: application to removal of divalent metals ions, J. Electroanal. Chem., 614 (2008) 31–40.
[34] M. Sugiura, M. Kikkawa, S. Urita, Carrier-mediated transport of rare earth ions through cellulose triacetate membranes, J. Membr. Sci., 42 (1989) 47–55.
[35] L.D. Nghiema, P. Mornanea, I.D. Potter, J.M. Perera, R.W. Cattrall, S.D. Kolev, Extraction and transport of metal ions and small organic compounds using polymer inclusion membranes (PIMs), J. Membr. Sci., 281 (2006) 7–41.
[36] I.C. McNeill, S. Ahmed, L. Memetea, Thermal degradation of vinyl acetate-methacrylic acid copolymer and homopolymers. I. An FTIR spectroscopic investigation of structural changes in the degrading material, Polym. Degrad. Stab., 47 (1995) 423–433.
[37] S.C. Christopher, F.P. Stephan, Y. Hu, W.A. Mark, P.C. Painter, M.M. Coleman, Infrared characterization and determination of self-association equilibrium constants for methacrylic acid copolymers, J. Macromol. Sci. Part B Phys., 39 (2000) 197–223.
[38] D.H. Grant, N. Grassie, The thermal decomposition of polymethacrylic acid, Polymer, 2 (1960) 125–134.